frontiers | Frontiers in Physics

TYPE Original Research
PUBLISHED 23 November 2023
DOI 10.3389/fphy.2023.1308136

OPEN ACCESS

EDITED BY
Kelly Schultz,
Lehigh University, United States

REVIEWED BY
Corina Stefania Drapaca,
The Pennsylvania State University (PSU), United States
Thomas Goudoulas,
Technical University of Munich, Germany

*CORRESPONDENCE
John C. P. Hollister,
jhollister@g.ucla.edu
H. Pirouz Kavehpour,
pirouz@seas.ucla.edu

RECEIVED 05 October 2023
ACCEPTED 13 November 2023
PUBLISHED 23 November 2023

CITATION
Hollister JCP, Wang AC, Kim W, Giza CC, Prins ML and Kavehpour HP (2023), Shear thinning behavior of cerebrospinal fluid with elevated protein or cellular concentration.
Front. Phys. 11:1308136.
doi: 10.3389/fphy.2023.1308136

Shear thinning behavior of cerebrospinal fluid with elevated protein or cellular concentration

John C. P. Hollister[1]*, Anthony C. Wang[2,3], Won Kim[2,3], Christopher C. Giza[2,4,5,6], Mayumi L. Prins[2,6,7] and H. Pirouz Kavehpour[1,8]*

[1]Department of Mechanical and Aerospace Engineering, University of California Los Angeles, Los Angeles, CA, United States, [2]Department of Neurosurgery, David Geffen School of Medicine, University of California Los Angeles, Los Angeles, CA, United States, [3]Department of Radiation Oncology, David Geffen School of Medicine, University of California Los Angeles, Los Angeles, CA, United States, [4]Department of Pediatrics, University of California Los Angeles, Los Angeles, CA, United States, [5]Interdepartmental Programs for Neuroscience and Biomedical Engineering, University of California Los Angeles, Los Angeles, CA, United States, [6]Steve Tisch BrainSPORT Program, University of California Los Angeles, Los Angeles, CA, United States, [7]Brain Injury Research Center, University of California Los Angeles, Los Angeles, CA, United States, [8]Department of Bioengineering, University of California Los Angeles, Los Angeles, CA, United States

Introduction: Cerebrospinal fluid (CSF) plays a crucial role in the maintenance of the central nervous system (CNS) by cushioning the brain, providing nutrients, removing interstitial waste, and maintaining homeostasis. Flow characteristics of CSF may significantly contribute to brain dynamics, injury mechanics, disease pathogenesis, and the functionality of the glymphatic system. Conventionally, CSF is considered to have very similar rheological properties to water and Newtonian behavior of CSF has been assumed, despite its complex composition, which can include proteins like albumin and tau, as well as cellular content such as blood.

Methods: Recent advances in rheological techniques allow for more accurate quantification of CSF characteristics and behavior. Here, we present an updated rheological characterization of CSF, including the impact of its cellular and proteinaceous constituents. CSF samples were tested for protein and cellular concentration. Using precision torsional rheometry and recently developed extensional rheology techniques, we show that CSF with elevated cellular or protein concentration exhibits significant non-Newtonian behavior, especially at low shear rates.

Results: Like other biological fluids, CSF with elevated cellular or protein concentration exhibits shear thinning behavior until reaching a steady state viscosity of approximately 1 mPa·s at shear rates greater than 10 s^{-1}. This shear thinning behavior becomes more pronounced with increasing concentration of its constituents. In extensional flow, CSF exhibited weakly non-Newtonian behavior, with an average extensional relaxation time of 0.14 ms. The extensional relaxation time is positively correlated to cellular concentration and significantly increased with elevated protein.

Discussion: Our results enhance the understanding of CSF rheology with significant implications for the analysis, modeling, and treatment of CSF-related processes.

KEYWORDS

shear thinning, cerebrospinal fluid, CSF, rheology, extensional, non-Newtonian

1 Introduction

Cerebrospinal fluid (CSF) is key to the protection and normal physiologic function of the central nervous system. In a typical adult, the volume of CSF is approximately 150 mL, most of which is produced in the ventricles of the brain, and flows into and through these ventricles, the subarachnoid spaces, and the brain parenchyma [1]. CSF is then re-absorbed into the venous system via arachnoid granulations, primarily through the superior sagittal sinus [2, 3]. CSF supplies nutrients and maintains homeostasis of the interstitial fluid environment of the brain. This function helps maintain normal neuronal function and removes metabolic by-products and interstitial waste like carbon dioxide and proteins such as amyloid-β and tau that could interfere with normal brain function [4, 5].

Conventionally, CSF is considered to be water-like, or is often simplified and approximated to have the properties of water [6]. However, due to the presence of proteins like albumin and tau, as well as cellular content including blood and immune cells [7], it is hypothesized that CSF actually exhibits significant non-Newtonian behavior, particularly at lower shear rates [8]. CSF from typical healthy humans contains 5,000–20,000 cells/mL and approximately 15–60 mg/dL of protein [7, 9]. However, the concentration of cells and protein can vary significantly with the condition of the patient [10]. Therefore, in order to fully describe CSF behavior, it is critically important to understand the impact of the various CSF constituents on its rheology.

With modern updated rheological techniques, a more accurate quantification of CSF rheology is possible. To our knowledge, the most comprehensive characterization of CSF rheology was performed by Bloomfield, et al., who, using a concentric cylinder rheometer, found that CSF is practically Newtonian with a viscosity similar to water [6]. They also found that the viscosity was independent of the contents of the CSF, and showed little-to-no correlation between cellular or protein concentration and viscosity. One significant gap, however, is that this paper only reported the CSF viscosity at shear rates between 150 s^{-1} and 1,500 s^{-1} and neglected lower shear rates. Shear rates within CSF are not always high [11], however, and low shear-rate behavior may be overlooked with the current knowledge.

The stress response of a Newtonian fluid such as water will vary linearly with shear rate, and therefore its viscosity will remain constant. A non-Newtonian fluid's stress response will vary non-linearly, and its viscosity may instead be a variable function of shear rate. Many biological fluids exhibit a shear thinning behavior, meaning that as shear rate increases, the apparent viscosity of the fluid decreases. It is hypothesized that this occurs due to the randomly oriented and dispersed polymeric and cellular contents of the fluid becoming disentangled and flowing more freely at higher shear rates. Blood is an example of a shear thinning biological fluid, in which the red blood cells form ordered aggregates called rouleaux [12]. These three-dimensional cell structures flow more freely than when randomly dispersed, and thus reduce the apparent viscosity of blood as a whole [13]. We hypothesize that a similar phenomenon may occur within CSF, especially when higher than normal protein and cellular content is present within the sample.

Extensional rheology is a growing field where the properties of fluids are analyzed as they are subjected to *extensional* strain rather than the more typical shear strain described above. In shear flow, the velocity gradient is perpendicular to the direction of the flow. In extensional flow, the velocity gradient is parallel to the flow direction. There are many applications where extensional strains are important, such as dripping phenomena and constricting or accelerating flow fields. In particular, the cross-linking and molecular interaction of polymers and proteins in solution cause fluids to exhibit non-Newtonian viscoelastic behaviors in extensional flow. Extensional methods have also been shown to be uniquely sensitive in measuring the influence of polymers and proteins within small volume dilute solutions [14, 15], making it appropriate for the characterization of biological fluids such as CSF in which cells and proteins may be relatively disperse and which may only be available in small volumes.

Both shear and extensional rheological behavior may contribute to many mechanical phenomena within the brain, especially in abnormal or clinical circumstances. For example, since viscosity is a measurement of a fluid's response to applied stress, the dynamics of the brain and the deformation experienced by brain tissue, especially during TBI or related injuries may be influenced by CSF rheology. Additionally, because the flow through shunts and their associated apparatuses can occur at relatively low shear rates, analysis of shunt function may be enhanced by understanding the shear rate dependent behavior of CSF [16]. Furthermore, CSF rheology may contribute to the mechanisms used to clear and expel waste, such as the hypothesized glymphatic system [4, 7, 17, 18]. Therefore, current and future CSF models may benefit from state-of-the-art rheological analysis. The goal of this research is to update the knowledge base of CSF rheological properties using state-of-the-art rheometry instruments and recently developed extensional rheology techniques, which will have significant implications for the understanding of the fluidic processes of the cranial system such as bulk CSF flow, injury mechanics, extracellular interstitial flow, and glymphatic clearance.

2 Materials and methods

2.1 CSF sample collection

Institutional Review Board exemption was confirmed prior to specimen collection. CSF was collected from patients at Ronald Reagan UCLA Hospital with in-dwelling external CSF drainage catheters. Indications for CSF diversion in these patients most commonly included trauma, hydrocephalus, hemorrhage, or infection.

2.2 Nexcelom cell counter

The total cellular concentration of each sample was measured using a Nexcelom Cellometer Auto 2000 (Nexcelom Bioscience, Lawrence MA, United States). Prior to testing, each CSF sample was appropriately diluted and dispensed in 20 μL increments to be read by the cellometer. The cellometer was set to the total cell concentration test, which counts all cells without debris and viability greater than 98%. Generally, each sample was diluted 2: 1 with phosphate buffer solution. In samples where the overlapping

cellular content caused counting errors, however, the samples were further diluted up to 20:1, in order to accurately count the cells on the slide.

2.3 Urine dipstick

Depending on the condition for which CSF drainage was required, CSF samples contained varying amounts of aqueous proteins. To quantify the relative proteinaceous composition of the samples, each was tested using a urine dipstick (LW Scientific, Lawrenceville GA, United States). The results of this test are quantified as Negative (no protein detected), Trace (<30 mg/dL), + (30–100 mg/dL), ++ (100–300 mg/dL), +++ (300–2000 mg/dL), and ++++ (>2000 mg/dL). Though this test does not identify the different proteins present within the sample, understanding their general relative effects will enhance the understanding of non-Newtonian behavior of CSF.

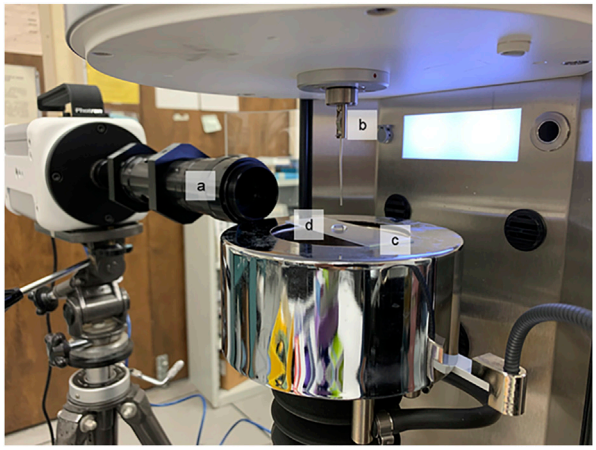

FIGURE 1
Micro-Extensional rheology test apparatus **(A)** Photron High-Speed camera, **(B)** Kruss K-100 tensiometer with 1 mm platinum probe, **(C)** hydrophobically treated surface, **(D)** liquid sample droplet.

2.4 Flow sweep

To investigate the shear-rate dependence of CSF rheology, a Discovery HR-3 rheometer with a recessed end concentric cylinder attachment (TA Instruments, New Castle DE, United States) was employed. As the expected viscosity of the CSF samples was estimated to be approximately 1–2 mPa·s (1–2 centipoise), the concentric cylinder attachment was chosen over a cone-and-plate configuration to avoid any confounding effects of surface tension on the sample's resistance to flow [19]. The rheometer operates by submerging a cylindrical probe (28 mm diameter) into the sample within a fixed concentric cylinder of known diameter (30 mm diameter). The sample fills the gap between the probe and cylinder wall. A motor within the instrument rotates the probe at a prescribed angular velocity and simultaneously measures the amount of torque required to maintain that velocity. Given the known geometry of the probe and concentric cylinder, this torque reading can be analyzed to measure a host of rheological properties.

Using the Discovery HR-3 rheometer with concentric cylinder attachment, a flow sweep was employed to investigate the shear-rate dependent behavior of CSF rheology. In this test, the probe rotates at a progression of prescribed angular velocities and thus produces prescribed shear rates. The stress response of the sample is calculated from the geometry of the rotating probe and the torque generated by the instrument to maintain the angular velocity.

For each CSF sample, 8 mL was tested at 37°C at shear rates varying from 0.3 to 300 s^{-1}. These limits were chosen based on the capabilities of the instrument [19], but only the behavior between 1 and 100 s^{-1} are reported below. For low viscosity fluids, low shear rate rheology may be influenced by interfacial effects such as surface tension, while high shear rate rheology may be influenced by secondary flow effects such as turbulence [19], causing the recorded data to exhibit erroneous behavior. Between 1 and 100 s^{-1}, the influence of these secondary effects is small, and the data can be considered reliable. Each data point was collected as a five second time average after thirty second equilibration period. The shear rate dependent viscosity data was collected and fit to a power law model (Eq. (1)), from which the infinite shear viscosity, μ_∞, and the flow behavior index (n-index), n, was calculated. *K* is the consistency index, which is an indicator of the fluid's viscosity. An n-index close to unity indicates a Newtonian fluid, while lower n-indices indicate shear thinning behavior.

$$\mu = \mu_\infty + K\dot{\gamma}^{(n-1)} \quad (1)$$

Analysis using the Casson model [20] for shear thinning fluid can be found in the Supplementary Material for this article.

2.5 Micro-extensional rheology

To analyze the extensional rheological properties of the CSF, we adapted a simple rheometric method to apply a large strain rate to the samples (Figure 1) [21]. A droplet, typically between 50 and 100 μL, was dispensed onto a hydrophobically treated substrate to create a domed droplet. Using a KRUSS tensiometer (K-100, KRUSS GmbH, Hamburg, Germany) in the Surface Tension setting, the droplet was penetrated with a 1 mm diameter platinum rod. The probe penetrated 0.5 mm into each sample and was quickly removed so that the surface of the sample was perturbed upward. Each sample was separated into three droplets, and each droplet was tested independently three times. Testing was performed at room temperature.

As the sample dripped from the probe, an elasto-capillary liquid bridge formed between the probe and the droplet. A high-speed camera (NOVA R2, PHOTRON USA INC., San Diego, United States) set to 20,000 frames per second and 1/25,000 s^{-1} shutter speed captured the evolution of the liquid bridge. The high-speed images were processed to analyze the evolution of the liquid bridge over time using a method adapted from Dinic et al [22]. The exponentially decaying portion of these data were fit to the following relationship (Eq. (2)) developed by Entov and Hinch [23], which describes the decay of the elastocapillary bridge that occurs during

TABLE 1 Summary of test results for each sample tested.

Sample	Protein	Cells/mL (×10^6)	Cell size (μm)	K (mPa·s)	μ_∞ (mPa·s)	n-index	λ_E (ms)
1[a]	+++	2.2	7.4	—	—	—	0.14
2[a]	Trace	0.4	11.9	—	—	—	0.13
3[a]	+++	396.0	10.7	—	—	—	0.13
4[a]	+	10.1	8.6	—	—	—	0.18
5[a]	++	408.0	11.2	—	—	—	0.15
6[a]	++	59.1	11.4	—	—	—	0.17
7	++	10.3	8.7	1.74	0.98	0.23	0.14
8	+	1.3	7.9	0.56	1.00	0.44	0.12
9	+++	5.6	10.7	2.08	0.95	0.48	0.13
10	++	1.9	7.8	1.04	0.91	0.24	0.13
11	Trace	1.5	11.2	0.91	0.90	1.00	0.12
12	+++	28.1	7.6	1.18	1.02	0.11	0.07
13	Trace	0.9	9	0.90	0.91	0.98	0.07
14	Negative	1.0	9.6	0.60	0.87	0.74	0.07
15	Trace	0.8	10.8	0.74	0.95	0.93	0.08
16	Trace	0.4	8.3	0.68	0.99	0.94	0.09
17	+++	12.1	9.2	0.76	0.94	0.34	0.09
18	+++	1.2	10.3	1.87	0.88	0.24	0.09
19	+	2.0	8.2	3.47	0.94	0.10	0.08
20	+++	275.0	11.2	3.44	1.32	0.25	0.35
21	Trace	3.2	9.1	0.66	0.93	0.79	0.11
22	++	3.8	8.1	2.27	0.89	0.14	0.12
23	Negative	3.1	8.6	0.89	0.92	1.01	0.14
24	++	30.9	8.7	1.26	0.93	0.24	0.18
25	++	25.9	10.7	1.14	0.95	0.45	0.19
26	++	10.2	9.4	0.71	0.92	0.64	0.20
27	+++	387.0	9.9	3.33	1.17	−0.16	0.19
28	+++	142.0	10.1	2.27	1.02	0.32	0.16
29[b]	+++	2300.0	11.2	4.74	2.53	0.67	0.35
30	Negative	1.7	8.6	0.93	0.94	0.53	0.12
31	++	54.1	7.3	0.38	0.85	0.74	0.14
32	+++	346.0	9.8	2.16	0.96	0.00	0.16
Average	**++**	**71.8**	**9.4**	**1.56**	**0.96**	**0.47**	**0.14**

[a]Samples 1–6 were not tested for shear rheology as the volume of these samples was too low (less than 8 mL).
[b]Sample 29 is an outlier approaching content of whole blood and is excluded from summary analysis.
Values are bold to highlight that they are averages of the overall data above it.

pinch-off of protein solutions. R_0, G_E, and σ are initial radius, elastic modulus, and surface tension of the fluid sample, respectively.

$$\frac{R(t)}{R_0} = \left(\frac{G_E R_0}{2\sigma}\right)^{1/3} exp\left(-\frac{t}{3\lambda_E}\right) \quad (2)$$

From this model, the extensional relaxation time (λ_E) of the elasto-capillary regime was calculated for each trial. Longer λ_E values correlate to higher protein concentration and greater cross-linking in the sample. Shorter relaxation times correlate to lower protein concentration [24].

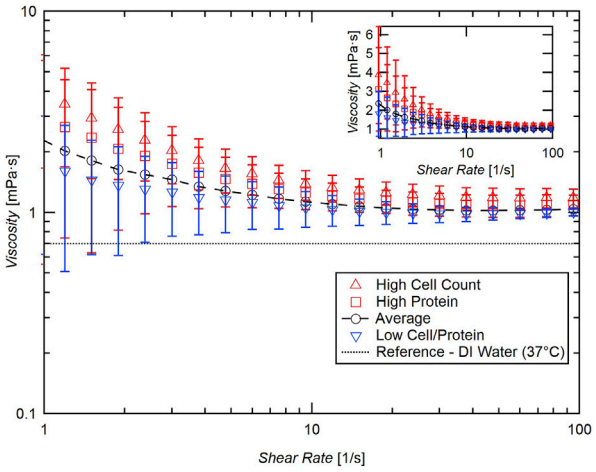

FIGURE 2
Summary of flow sweep test of samples with high cellular concentration (red triangles, >10^7 cells/mL), high protein (red squares, >30 mg/dL), and relatively low cellular/protein concentration (blue inverted triangles, <10^6 cells/mL, <30 mg/dL blue inverted triangles). Inset: semilog plot of data with linear viscosity axis.

3 Results

3.1 Sample characteristics

Thirty-two samples were collected and tested for cellular concentration and protein concentration (Table 1). While all samples exhibited some cellular content, half of the samples (16 of 32) showed obvious signs of hemorrhage, with cellular concentration greater than 10^7 cells/mL. One sample (sample 29) was an outlier and had cellular concentration approaching whole blood, representing an extreme case. Five samples had cellular concentrations low enough to approach that of normal CSF (<1 × 10 [6] cell/mL), but should still be considered elevated relative to normal CSF. Twenty samples were found to have elevated protein concentration. Eleven had protein content greater than 300 mg/dL, and another nine had samples greater than 100 mg/dL. The assessment of protein concentration using the urine dipstick is somewhat subjective, so great care was taken to record a conservative estimate of protein concentration in each case.

3.2 Flow sweep

When significant cellular or protein concentration was present within the sample, the sample exhibited shear thinning behavior, especially at low shear rates below 10 s^{-1}. This shear thinning behavior generally dissipated approaching 100 s^{-1}, at which point all samples behaved as a Newtonian fluid. When both cellular and protein concentration were relatively low, however, the sample behaved comparatively more like a Newtonian Fluid throughout testing. The results of these tests are displayed in Figure 2 and Table 1.

Though the samples exhibited shear thinning behavior at low shear rates, the findings of previous studies are confirmed for moderate to higher shear rates. Each sample data set was fit to Eq. 1 and the infinite shear viscosity (μ_∞) was calculated. The average overall μ_∞ for these samples is very close to distilled water, 1.0 mPa·s. Although there is a positive correlation between viscosity and cellular concentration, the effect is small, and a great change in cellular content is necessary to significantly influence the viscosity of CSF (Figure 3).

Elevated protein content (>30 mg/dL) similarly shows a weakly significant increase in viscosity (p-value 0.08), and only the group measuring greater than 300 mg/dL individually exhibited a significantly elevated viscosity when compared to the protein-negative group (p = 0.05) (Figure 3). Though the measurement was statistically significant, the difference in means is only roughly 0.1 mPa·s (0.9 vs. 1.0 mPa·s).

The shear thinning behavior was quantified by fitting the viscosity and shear rate data to Eq. 1 and extracting the flow behavior index (n-index), n. n-values close to unity indicate a Newtonian fluid, while lower n-values indicate shear thinning behavior. n-values approaching zero indicate steeper decreases in viscosity at lower shear rates.

A negative correlation between the n-index and cellular content of the CSF is observed, with increasing cellular concentration indicating more significant shear thinning behavior (Figure 4). Samples with elevated protein content also exhibited significantly greater shear thinning behavior, as the n-index for these samples was significantly lower than samples with either negative or trace protein (p < 0.001) (Figure 4).

3.3 Micro-extensional rheology

All samples exhibited weak, but non-zero non-Newtonian extensional behavior (Figure 5). The average extensional relaxation time for all samples tested was 0.14 ms with a slight positive correlation to both cellular and protein concentration (Figure 6). While all samples showed a clear liquid bridge characteristic of proteinaceous solutions, in many samples, this structure only lasted a few frames, or about 100–300 µs. One sample whose content approached that of whole blood, however, exhibited clear beads-on-a-string phenomena (Figure 7), indicative of high flow-induced protein entanglement [25].

4 Discussion

These results empirically demonstrate non-Newtonian behavior of CSF, especially in the presence of elevated cellular or protein concentration. One glaring weakness in the existing literature on CSF rheology are that prior studies have centrifuged CSF to characterize the underlying fluid behavior. We opted instead to characterize the extracted CSF sample as a whole, to better reflect the *in vivo* condition. We sought a variety of clinical conditions, and quantified the proportion of the cellular and protein constituents of the samples, to understand their relative impact on CSF rheology. With higher cellular and protein concentrations and lower shear rates, significant shear thinning behavior was observed, especially at shear rates below 10 s^{-1}. Although the results and conclusions from these data are limited, they have broad applicability to clinical

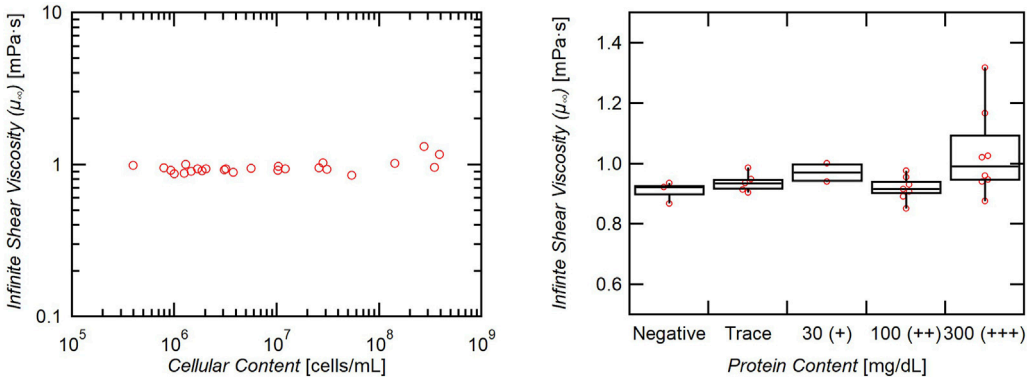

FIGURE 3
Effect of cellular and protein content on infinite shear viscosity. Viscosity increases minimally with increasing cellular content (slope = 6×10^{-13}), and only samples with 300+ mg/dL of protein exhibited a significantly increased viscosity ($p = 0.05$).

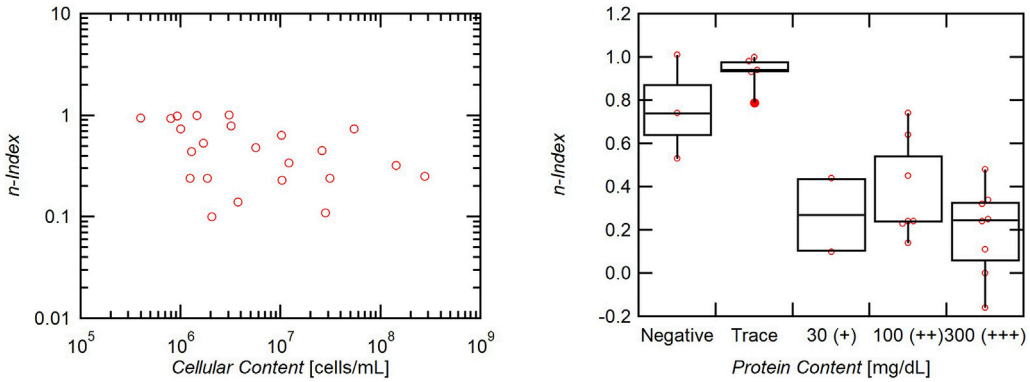

FIGURE 4
Effect of cellular and protein content on n-index. Increased cells indicate a lower n-index and therefore greater non-Newtonian shear thinning behavior. Increased protein has a strong effect on n-index as elevated protein correlates with lower n-indices and greater shear thinning behavior.

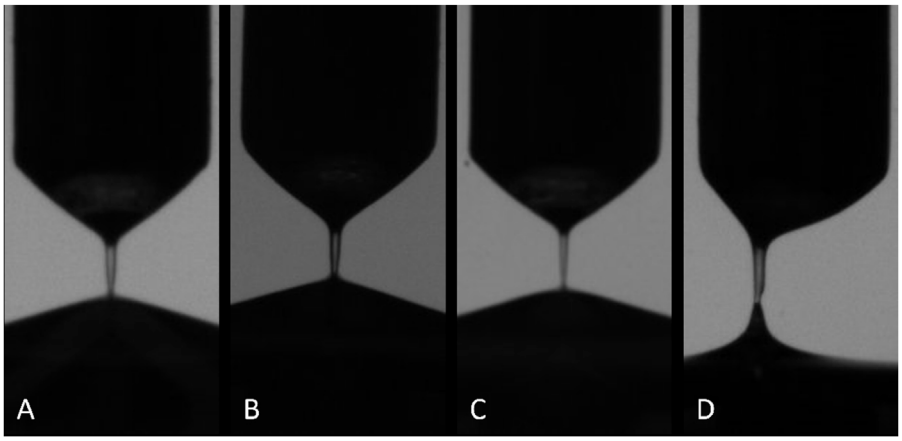

FIGURE 5
Examples of elasto-capillary bridge observed in all samples. Samples pictured in **(A–D)** represent increasing cellular and protein content as well as increasing extensional relaxation time. Sample pictured in **(D)** is a statistical outlier, and exhibited an average relaxation time approximately three times longer than the others.

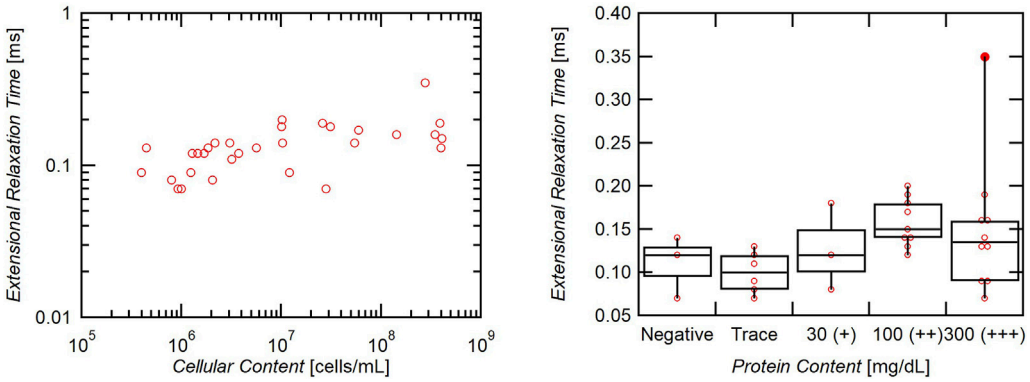

FIGURE 6
Effect of cellular and protein content on extensional relaxation time. Cellular content has a positive correlation to extensional relaxation time (slope = 1.7×10^{-10}). Samples with elevated protein (>30 mg/dL) also exhibited significantly higher extensional relaxation times ($p = 0.005$).

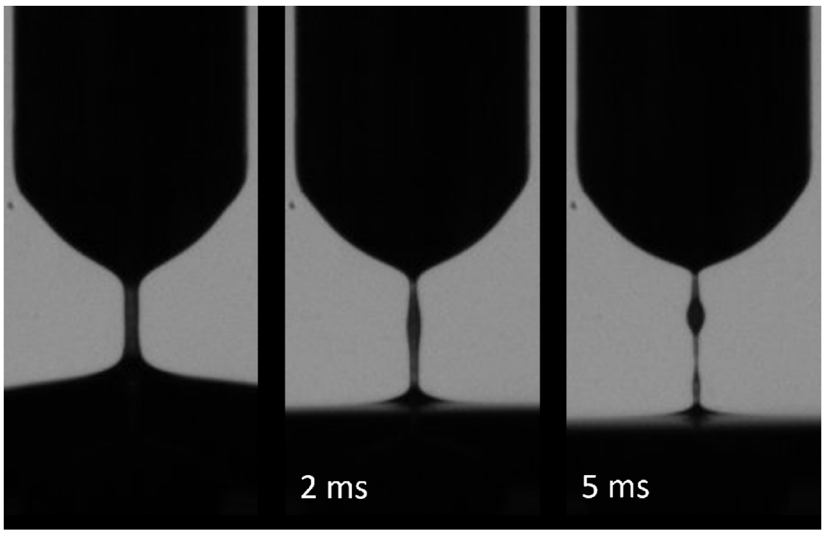

FIGURE 7
Outlier CSF sample with cellular content approaching blood (3×10^9 cells/mL). Elasto-capillary bridge persisted for longer than all other samples and exhibited beads-on-a-string morphology indicating high protein interactions. Sample is unique but represents an extreme hemorrhage.

situations when normal CSF conditions cannot necessarily be assumed.

Another important weakness in the existing literature on CSF rheology is that shear rates studied have largely been relatively high and have neglected lower shear rates that may be relevant to clinical applications such as shunts or the glymphatic system. In our studies, at higher shear rates, CSF indeed exhibited Newtonian behavior with a viscosity close to that of distilled water. Furthermore, when cellular and protein concentrations were relatively low, the CSF samples also exhibited behavior closer to Newtonian, even at low shear rates. These results confirm that bulk flow of healthy CSF can generally be considered Newtonian, and to approximate its viscosity to water may be appropriate. However, at lower shear rates, as in stagnation flow or creeping flow, the non-Newtonian behavior of CSF must be considered, especially in instances where cellular or protein concentration may be abnormally or locally elevated.

For example, flow through CSF shunts implanted to relieve hydrocephalus can be very slow, with shear rates on the order of 1 s^{-1}. In addition, the presence of the indwelling hardware is known to increase the cellular and protein content of the CSF in these patients [26]. Therefore, the analysis of shunt function would benefit from the consideration of non-Newtonian behavior at low shear rates. Another example is where CSF interacts with other brain constituents [27]—in the interstitial spaces of brain parenchyma, the perivascular spaces, the arachnoid granulations adjacent to the venous sinuses, and the hypothesized glymphatic system, which pulses CSF through interstitial space to clear waste resulting from normal neuronal function. This transported waste may change the local composition of CSF such that it exhibits more significant non-Newtonian behavior. Furthermore, the proposed glymphatic pathway is characterized by low velocity flow of CSF [28], which therefore may exhibit significant non-Newtonian behavior. As more

work is done to characterize the glymphatic pathway, it is imperative that non-Newtonian behavior of the transport media be considered. Finally, CSF reabsorption is hypothesized to occur with contributions from both pressure and osmotic gradients, again at very low velocity flow [29, 30].

In extensional flow, the behavior of CSF is not greatly influenced by its constituents, except in extreme cases. While all samples exhibited measurable non-Newtonian behavior, characterized by a short-duration elasto-capillary bridge, only two had significantly elevated extensional relaxation times. In one of these samples, the cellular and protein concentration approached that of whole blood, and should be considered an extreme case. In the majority of samples tested, the extensional relaxation time was relatively short, approximately 0.14 ms. To benchmark this relaxation time, it is higher than a Tau solution tested by Hosseini, et. al., and 10 mg/mL 35 kDa PEO (0.03 ms) [15]. It is lower, however, than hypersonically extracted vitreous solution (0.37 ms) [21] and 10 mg/mL 100 kDa PEO solution (0.67 ms) [15]. Non-Newtonian extensional behavior is significant when the duration of the extensional phenomenon is similar to the relaxation time. Therefore, extensional non-Newtonian behavior should be considered in short duration extensional processes, on the order of 0.1 ms.

The shear rate data presented in the flow sweep section of this report are limited in scope, and knowledge of this function will be enhanced by further measuring the low shear rate non-Newtonian behavior of CSF. Below 1 s^{-1}, the shear thinning behavior appeared to continue, though the data approaches the limit of our instrument's capabilities. More accurate descriptions of CSF non-Newtonian behavior could therefore be achieved with more sensitive instrumentation, including lower shear rate and yield stress behavior. Similarly, above 100 s^{-1}, secondary flow effects were significant, and data collected above this range are unreliable. Therefore, we were unable to achieve a continuous shear rate ramp to higher shear rates in the same sample without changing the instrumentation part way through testing. Having this continuous data would further confirm the Newtonian behavior of CSF at higher shear rates, as well as improve the quantification of the shear thinning behavior at lower shear rates.

In summary, we have demonstrated for the first time that CSF with elevated cellular or protein concentration behaves as a non-Newtonian fluid, especially at low shear rates. At high shear rates, it is confirmed that CSF behaves as a Newtonian fluid regardless of constituent concentration, with a viscosity similar to distilled water. In extensional flow, CSF exhibits measurable non-Newtonian behavior, but the effect is relatively weak and is independent of the cellular and protein concentration of the sample, except in extreme circumstances. These findings have broad implications for the characterization of CSF and CSF-related processes, and its non-Newtonian behavior should be considered when analyzing the fluid dynamics of CSF in a wide variety of physiologic and pathologic conditions.

Data availability statement

The raw data supporting the conclusion of this article will be made available by the authors, without undue reservation.

Ethics statement

The studies involving humans were approved by Gina Pendergrass, MIRB3 Administrator, UCLA. The studies were conducted in accordance with the local legislation and institutional requirements. The human samples used in this study were acquired from a by-product of routine care or industry. Written informed consent for participation was not required from the participants or the participants' legal guardians/next of kin in accordance with the national legislation and institutional requirements.

Author contributions

JH: Conceptualization, Data curation, Formal Analysis, Investigation, Methodology, Project administration, Resources, Validation, Visualization, Writing–original draft, Writing–review and editing. AW: Writing–review and editing, Resources. WK: Writing–review and editing. CG: Writing–review and editing, Funding acquisition. MP: Funding acquisition, Writing–review and editing. HK: Funding acquisition, Writing–review and editing, Conceptualization, Project administration, Supervision, Visualization.

Funding

The author(s) declare financial support was received for the research, authorship, and/or publication of this article. This work was partially supported by the UCLA Brain Injury Research Center (BIRC).

Conflict of interest

The authors declare that the research was conducted in the absence of any commercial or financial relationships that could be construed as a potential conflict of interest.

Publisher's note

Supplementary material

The Supplementary Material for this article can be found online at: https://www.frontiersin.org/articles/10.3389/fphy.2023.1308136/full#supplementary-material

References

1. Telano LN, Baker S Physiology, cerebral spinal fluid. In: *StatPearls [Internet]*. Treasure Island, FL: StatPearls Publishing (2023).

2. Sakka L, Coll G, Chazal J Anatomy and physiology of cerebrospinal fluid. *Eur Ann Otorhinolaryngol Head Neck Dis* (2011) 128:309–16. doi:10.1016/j.anorl.2011.03.002

3. Brinker T, Stopa E, Morrison J, Klinge P A new look at cerebrospinal fluid circulation. *Fluids and Barriers of the CNS* (2014) 11:10. doi:10.1186/2045-8118-11-10

4. Kelley DH, Thomas JH Cerebrospinal fluid flow. *Annu Rev Fluid Mech* (2023) 55: 237–64. doi:10.1146/annurev-fluid-120720-011638

5. Kaur J, Fahmy LM, Davoodi-Bojd E, Zhang L, Ding G, Hu J, et al. Waste clearance in the brain. *Front Neuroanat* (2021) 15:665803. doi:10.3389/fnana.2021.665803

6. Bloomfield IG, Johnston IH, Bilston LE Effects of proteins, blood cells and glucose on the viscosity of cerebrospinal fluid. *PNE* (1998) 28:246–51. doi:10.1159/000028659

7. Spector R, Robert Snodgrass S, Johanson CE A balanced view of the cerebrospinal fluid composition and functions: focus on adult humans. *Exp Neurol* (2015) 273:57–68. doi:10.1016/j.expneurol.2015.07.027

8. Wang C Correlation of the friction factor for turbulent pipe flow of dilute polymer solutions. *Ind Eng Chem Fund* (1972) 11:546–51. doi:10.1021/i160044a019

9. Seehusen DA, Reeves MM, Fomin DA Cerebrospinal fluid analysis. *afp* (2003) 68: 1103–8.

10. Brydon HL, Hayward R, Harkness W, Bayston R Does the cerebrospinal fluid protein concentration increase the risk of shunt complications? *Br J Neurosurg* (1996) 10:267–74. doi:10.1080/02688699650040124

11. Eide PK, Valnes LM, Lindstrøm EK, Mardal K-A, Ringstad G Direction and magnitude of cerebrospinal fluid flow vary substantially across central nervous system diseases. *Fluids and Barriers of the CNS* (2021) 18:16. doi:10.1186/s12987-021-00251-6

12. Nader E, Skinner S, Romana M, Fort R, Lemonne N, Guillot N, et al. Blood rheology: key parameters, impact on blood flow, role in sickle cell disease and effects of exercise. *Front Physiol* (2019) 10:1329. doi:10.3389/fphys.2019.01329

13. Cherry EM, Eaton JK Shear thinning effects on blood flow in straight and curved tubes. *Phys Fluids* (2013) 25:073104. doi:10.1063/1.4816369

14. Dinic J, Zhang Y, Jimenez LN, Sharma V Extensional relaxation times of dilute, aqueous polymer solutions. *ACS Macro Lett* (2015) 4:804–8. doi:10.1021/acsmacrolett.5b00393

15. Hosseini H, Rangchian A, Prins ML, Giza CC, Ruberti JW, Kavehpour HP Probing flow-induced biomolecular interactions with micro-extensional rheology: tau protein aggregation. *J Biomech Eng.-Trans ASME* (2020) 142:034501. doi:10.1115/1.4046330

16. Kadowaki C, Hara M, Numoto M, Takeuchi K, Saito I CSF shunt physics: factors influencing inshunt CSF flow. *Child's Nerv Syst* (1995) 11:203–6. doi:10.1007/bf00277654

17. Siyahhan B, Knobloch V, de Zélicourt D, Asgari M, Schmid Daners M, Poulikakos D, et al. Flow induced by ependymal cilia dominates near-wall cerebrospinal fluid dynamics in the lateral ventricles. *J R Soc Interf* (2014) 11:20131189. doi:10.1098/rsif.2013.1189

18. Rasmussen MK, Mestre H, Nedergaard M Fluid transport in the brain. *Physiol Rev* (2022) 102:1025–151. doi:10.1152/physrev.00031.2020

19. Ewoldt RH, Johnston MT, Caretta LM Experimental challenges of shear rheology: how to avoid bad data. In: Spagnolie SE, editor. *Complex fluids in biological systems: experiment, theory, and computation*. Springer (2015). p. 207–41. doi:10.1007/978-1-4939-2065-5_6

20. Casson NA Flow equation for pigment-oil suspensions of the printing ink type. *Rheology Disperse Syst* (1959) 84–104.

21. Hollister JCP, Rodriguez M, Hosseini H, Papour A, Hubschman JP, Kavehpour HP. Ultrasonic vitrectomy performance assessment using micro-extensional rheology. *Translational Vis Sci Tech* (2023) 12:24. doi:10.1167/tvst.12.2.24

22. Dinic J, Jimenez LN, Sharma V Pinch-off dynamics and dripping-onto-substrate (DoS) rheometry of complex fluids. *Lab Chip* (2017) 17:460–73. doi:10.1039/c6lc01155a

23. Entov VM, Hinch EJ Effect of a spectrum of relaxation times on the capillary thinning of a filament of elastic liquid. *J Non-Newtonian Fluid Mech* (1997) 72:31–53. doi:10.1016/s0377-0257(97)00022-0

24. Dinic J, Sharma V Macromolecular relaxation, strain, and extensibility determine elastocapillary thinning and extensional viscosity of polymer solutions. *Proc Natl Acad Sci* (2019) 116:8766–74. doi:10.1073/pnas.1820277116

25. Clasen C, Eggers J, Fontelos MA, Li J, McKINLEY GH The beads-on-string structure of viscoelastic threads. *J Fluid Mech* (2006) 556:283–308. doi:10.1017/s0022112006009633

26. Wilhelmy F, Krause M, Schob S, Merkenschlager A, Wachowiak R, Härtig W, et al. Cerebrospinal fluid protein concentrations in hydrocephalus. *Children* (2023) 10:644. doi:10.3390/children10040644

27. Thomas JH Fluid dynamics of cerebrospinal fluid flow in perivascular spaces. *J R Soc Interf* (2019) 16:20190572. doi:10.1098/rsif.2019.0572

28. Mestre H, Tithof J, Du T, Song W, Peng W, Sweeney AM, et al. Flow of cerebrospinal fluid is driven by arterial pulsations and is reduced in hypertension. *Nat Commun* (2018) 9:4878. doi:10.1038/s41467-018-07318-3

29. Krishnamurthy S, Li J New concepts in the pathogenesis of hydrocephalus. *Transl Pediatr* (2014) 3:185–94. doi:10.3978/j.issn.2224-4336.2014.07.02

30. Atchley TJ, Vukic B, Vukic M, Walters BC Review of cerebrospinal fluid physiology and dynamics: a call for medical education reform. *Neurosurgery* (2022) 91:1–7. doi:10.1227/neu.0000000000002000